

Anomalous Form Factor of the Neutral Pion in Extended AdS/QCD Model with Chern-Simons Term

H. R. Grigoryan^{1,2} and A. V. Radyushkin^{1,3,4}

¹*Thomas Jefferson National Accelerator Facility, Newport News, VA 23606, USA*

²*Physics Department, Louisiana State University, Baton Rouge, LA 70803, USA*

³*Physics Department, Old Dominion University, Norfolk, VA 23529, USA*

⁴*Laboratory of Theoretical Physics, JINR, Dubna, Russian Federation*

We propose an extension of the hard-wall AdS/QCD model by including the Chern-Simons term required to reproduce the chiral anomaly of QCD. In the framework of this holographic model, we study the vertex function $F_{\pi\gamma^*\gamma^*}(Q_1^2, Q_2^2)$ which accumulates information about the coupling of the pion to two (in general virtual) photons. We calculate the slope of the form factor with one real and one slightly virtual photon and show that it is close to experimental findings. We analyze the formal limit of large virtualities and establish that predictions of the holographic model analytically (including nontrivial dependence on the ratio of photon virtualities) coincide with those of perturbative QCD calculated for the asymptotic form of the pion distribution amplitude. We also investigate the generalized VMD structure of $F_{\pi\gamma^*\gamma^*}(Q_1^2, Q_2^2)$ in the extended AdS/QCD model.

PACS numbers: 11.25.Tq, 11.10.Kk, 11.15.Tk 12.38.Lg

I. INTRODUCTION

The form factor $F_{\gamma^*\gamma^*\pi^0}(Q_1^2, Q_2^2)$ describing the coupling of two (in general, virtual) photons with the lightest hadron, the pion, plays a special role in the studies of exclusive processes in quantum chromodynamics (QCD). When both photons are real, the form factor $F_{\gamma^*\gamma^*\pi^0}(0, 0)$ determines the rate of the $\pi^0 \rightarrow \gamma\gamma$ decay, and its value at this point is deeply related to the axial anomaly [1]. Because of this relation, the $\gamma^*\gamma^*\pi^0$ form factor was an object of intensive studies since the 60's [2]-[6].

At large photon virtualities, its behavior was studied [7, 8, 9] within perturbative QCD (pQCD) factorization approach for exclusive processes [7, 10, 11]. Since only one hadron is involved, the $\gamma^*\gamma^*\pi^0$ form factor has the simplest structure for pQCD analysis, with the nonperturbative information about the pion accumulated in the pion distribution amplitude $\varphi_\pi(x)$ introduced in Refs. [12, 13]. Another simplification is that the short-distance amplitude for $\gamma^*\gamma^*\pi^0$ vertex is given, at the leading order, just by a single quark propagator. Theoretically, most clean situation is when both photon virtualities are large, but the experimental study of $F_{\gamma^*\gamma^*\pi^0}(Q_1^2, Q_2^2)$ in this regime through the $\gamma^*\gamma^* \rightarrow \pi^0$ process is very difficult due to very small cross section.

The leading-twist pQCD factorization, however, works even if one of the photons is real or almost real. Furthermore, this kinematics is amenable to experimental investigation through the $\gamma\gamma^* \rightarrow \pi^0$ process at e^+e^- colliders. Comparison of the data obtained by CELLO [14] and CLEO [15] collaborations with the original leading [7, 8] and next-to-leading order [16, 17, 18, 19] pQCD predictions amended by later studies [20, 21] that incorporate a more thorough treatment of the real photon channel using the light-cone QCD sum rule ideas provided important information about the shape of the pion distribution amplitude $\varphi_\pi(x)$ (for the most recent review see

[22]). The momentum dependence of $F_{\gamma^*\gamma^*\pi^0}(0, Q^2)$ form factor was also studied in various models of nonperturbative QCD dynamics (see, e.g., [23]-[37] and references therein).

In the present paper, our goal is to extend the holographic dual model of QCD to incorporate the anomalous $F_{\gamma^*\gamma^*\pi^0}(Q_1^2, Q_2^2)$ form factor. During the last few years applications of gauge/gravity duality [38] to hadronic physics attracted a lot of attention, and various holographic dual models of QCD were proposed in the literature (see, e.g., [39]-[59]). These models were able to incorporate such essential properties of QCD as confinement and dynamical chiral symmetry breaking, and also to reproduce many of the static hadronic observables (decay constants, masses), with values rather close to the experimental ones.

As the basis for our extension, we follow the holographic approach of Refs. [43, 45], and then intend to proceed along the lines of formalism outlined in our recent papers [60, 61], where it was first applied to form factors and wave functions of vector mesons [60, 62] (tensor form factors of vector mesons were considered in [63]) and later [61] to the pion electromagnetic form factor. However, a straightforward application of the approach of Refs. [43, 45, 60, 61] to $F_{\gamma^*\gamma^*\pi^0}(Q_1^2, Q_2^2)$ form factor gives a vanishing result. There are two obvious reasons for such an outcome.

First, the five-dimensional (5D) gauge fields $B^a(x, z)$ in the AdS/QCD lagrangian of Refs. [43, 45] are only dual to the 4D isovector currents $J^a(x)$. On the other hand, a nonzero result for the matrix element $\langle 0 | J_{EM}^\mu J_{EM}^\nu | \pi^0 \rangle$ defining the $F_{\gamma^*\gamma^*\pi^0}(Q_1^2, Q_2^2)$ form factor may be obtained only when the electromagnetic currents J_{EM}^μ, J_{EM}^ν have both isovector and isoscalar components, which is the case in two-flavor QCD, but not in the holographic models of Refs. [43, 45].

Thus, we need an AdS/QCD model that includes gauge fields in the 5D bulk which are dual to both isovector and

isoscalar currents. The natural way to do this is to extend the gauge group $SU(2)_L \otimes SU(2)_R$ in the bulk up to $U(2)_L \otimes U(2)_R$. After explicit separation of the isosinglet and isovector parts, the new 5D field can be written as $B_\mu = t^a B_\mu^a + \mathbb{1} \frac{\hat{B}_\mu}{2}$, with $\mathbb{1}$ being the unity matrix. The \hat{B} part is dual to 4D isosinglet vector current.

Even after this modification, the AdS/QCD action gives zero result for the correlator $\langle 0 | J_\mu^{\{I=1\}} J_\nu^{\{I=0\}} J_\alpha^A | 0 \rangle$ involving two vector currents $J_\mu^{\{I=1\}}$, $J_\nu^{\{I=0\}}$ and the axial current J_α^A (that has nonzero projection onto the pion state). To bring in the anomalous amplitude into the model, the next step (similar to [67]) is to add a Chern-Simons term [68] to the action. After these extensions, the calculation of the $F_{\gamma^* \gamma^* \pi^0}(Q_1^2, Q_2^2)$ form factor may be performed using the methods developed in Refs. [60, 61].

The paper is organized in the following way. We start by recalling, in Section II, the basics of the hard-wall model, in particular, the form of the action given in Ref. [43] and our results [61] for the pion wave function. In Section III, we consider the generalization of the AdS/QCD model that includes isoscalar fields and Chern-Simons term. Using this extended model we describe the calculation of the $F_{\gamma^* \gamma^* \pi^0}(Q_1^2, Q_2^2)$ form factor and express it in terms of the pion wave function and two bulk-to-boundary propagators for the vector currents describing EM sources. In Section IV, we study the results obtained within the extended AdS/QCD model with one real and one slightly virtual photon and calculate the value of the Q^2 -slope of the form factor. We also discuss

the formal limit of large photon virtualities, and compare these results to those obtained in pQCD. In Section V, we study the generalized VMD structure of the AdS/QCD model expression for the $F_{\gamma^* \gamma^* \pi^0}(Q_1^2, Q_2^2)$ form factor. Finally, we summarize the paper.

II. BASICS OF HARD-WALL MODEL

In the holographic model, QCD resonances correspond to Kaluza-Klein type excitations of the sliced AdS₅ space with the metric

$$g_{MN} dx^M dx^N = \frac{1}{z^2} (\eta_{\mu\nu} dx^\mu dx^\nu - dz^2) , \quad (1)$$

where $\eta_{\mu\nu} = \text{Diag}(1, -1, -1, -1)$ and $\mu, \nu = (0, 1, 2, 3)$, $M, N = (0, 1, 2, 3, z)$. The basic prescription is that there is a correspondence between the 4D vector and axial-vector currents and 5D gauge fields $V_\mu^a(x, z)$ and $A_\mu^a(x, z)$. Furthermore, since the gauge invariance corresponding to the axial-vector current is spontaneously broken in the 5D background, the longitudinal component of the axial-vector field becomes physical and related to the pion field.

A. AdS/QCD action

The action of the holographic model of Ref. [43] can be written in the form

$$S_{\text{AdS}}^B = \text{Tr} \int d^4x \int_0^{z_0} dz \left[\frac{1}{z^3} (D^M X)^\dagger (D_M X) + \frac{3}{z^5} X^\dagger X - \frac{1}{8g_5^2 z} (B_{(L)}^{MN} B_{(L)MN} + B_{(R)}^{MN} B_{(R)MN}) \right] , \quad (2)$$

where $DX = \partial X - iB_{(L)}X + iXB_{(R)}$, $(B_{(L,R)} = V \pm A)$ and $X(x, z) = v(z)U(x, z)/2$ is taken as a product of the chiral field $U(x, z) = \exp[2it^a \pi^a(x, z)]$ (as usual, $t^a = \sigma^a/2$, with σ^a being Pauli matrices) and the function $v(z) = (m_q z + \sigma z^3)$ containing the chiral symmetry breaking parameters m_q and σ , with m_q playing the role of the quark mass and σ that of the quark condensate.

In general, one can write $A = A_\perp + A_\parallel$, where A_\perp and A_\parallel are transverse and longitudinal components of the axial-vector field. The spontaneous symmetry breaking causes A_\parallel to be physical and associated with the Goldstone boson, pion in this case. The longitudinal component is written in the form:

$$A_{\parallel M}^a(x, z) = \partial_M \psi^a(x, z) . \quad (3)$$

Then $\psi^a(x, z)$ corresponds to the pion field. This Higgs-like mechanism breaks the axial-vector gauge invariance by bringing a z -dependent mass term in the A -part of the lagrangian.

Varying the action with respect to the transverse gauge fields V_μ^a and $A_{\perp\mu}^a$ gives equations of motion for these fields describing (*via* the holographic correspondence) the physics of vector and axial-vector mesons. Variation with respect to $A_{\parallel\mu}^a$ and A_z^a gives two coupled equations for the chiral field $\pi^a(x, z)$ and the pion field $\psi^a(x, z)$. It is convenient to work in Fourier representation, where $\tilde{V}_\mu^a(p, z) = \tilde{V}_\mu^a(p) \mathcal{V}(p, z)$ is the Fourier transform of $V_\mu^a(x, z)$, and $\tilde{A}_\mu^a(p, z)$ is the Fourier transform of $A_\mu^a(x, z)$.

B. Vector channel

The vector bulk-to-boundary propagator

$$\mathcal{V}(p, z) = g_5 \sum_{m=1}^{\infty} \frac{f_m \psi_m^V(z)}{-p^2 + M_m^2} \quad (4)$$

has the bound-state poles for $p^2 = M_n^2$, with the resonance masses $M_n = \gamma_{0,n}/z_0$ ($\gamma_{0,n}$ is n^{th} zero of the Bessel function $J_0(x)$) determined by the eigenvalues of the equation of motion

$$\partial_z \left[\frac{1}{z} \partial_z \psi_n^V(z) \right] + \frac{1}{z} M_n^2 \psi_n^V(z) = 0, \quad (5)$$

subject to boundary conditions $\psi_n^V(0) = \partial_z \psi_n^V(z_0) = 0$. The eigenfunctions of this equation give the “ ψ ” wave functions

$$\psi_n^V(z) = \frac{\sqrt{2}}{z_0 J_1(\gamma_{0,n})} z J_1(M_n z) \quad (6)$$

for the relevant resonances. The coupling constants f_n are determined from the ψ wave functions through

$$f_n = \frac{1}{g_5} \left[\frac{1}{z} \partial_z \psi_n^V(z) \right]_{z=0} = \frac{\sqrt{2} M_n}{g_5 z_0 J_1(\gamma_{0,n})}. \quad (7)$$

In Ref. [60], we introduced “ ϕ wave functions”

$$\phi_n^V(z) \equiv \frac{1}{M_n z} \partial_z \psi_n^V(z) = \frac{\sqrt{2}}{z_0 J_1(\gamma_{0,n})} J_0(M_n z), \quad (8)$$

which give the couplings $g_5 f_n / M_n$ as their values at the origin, just like the ($L = 0$) bound state wave functions in quantum mechanics. Moreover, these functions satisfy Dirichlet b.c. $\phi_n^V(z_0) = 0$. Physically, the ψ^V wave functions describe the vector bound states in terms of the vector potential V_μ , while the ϕ^V wave functions describe them in terms of the field-strength tensor $\partial_z V_\mu = V_{z\mu}$ (we work in the axial gauge, where $V_z = 0$).

An essential ingredient of form factor formulas is the vector bulk-to-boundary propagator $\mathcal{J}(Q, z) \equiv \mathcal{V}(iQ, z)$ taken at a spacelike momentum p with $p^2 = -Q^2$. It can be written in a closed form as

$$\mathcal{J}(Q, z) = Qz \left[K_1(Qz) + I_1(Qz) \frac{K_0(Qz_0)}{I_0(Qz_0)} \right]. \quad (9)$$

The function $\mathcal{J}(Q, z)$ satisfies the relations $\mathcal{J}(Q, 0) = 1$, $\mathcal{J}(0, z) = 1$ and $\partial_z \mathcal{J}(Q, z_0) = 0$.

C. Pion channel

An important achievement of the hard-wall model of Ref. [43] is its compliance with the Gell-Mann–Oakes–Renner relation $m_\pi^2 \sim m_q$ that produces a massless pion in the $m_q = 0$ limit. The fits of Ref. [43] give very small value $m_q \sim 2$ MeV for the “quark mass” parameter m_q , so it makes sense to resort to the chiral $m_q = 0$ limit, which has an additional advantage that solutions of equations of motion in this case can be found analytically. The pion wave function $\psi(z)$ is introduced through the longitudinal part of the axial-vector field:

$$\tilde{A}_{\parallel\mu}^a(p, z) = \frac{p_\mu p^\alpha}{p^2} \tilde{A}_\alpha^a(p) \psi(z), \quad (10)$$

The bulk-to-boundary part $\pi(z)$ of the $\pi^a(z)$ field, in the zeroth order of the m_π^2 expansion proposed in Ref [43] tends to -1 . Then the equation for $\Psi(z) \equiv \psi(z) - \pi(z)$ is exactly solvable, with the result

$$\Psi(z) = z \Gamma(2/3) \left(\frac{\alpha}{2} \right)^{1/3} \left[I_{-1/3}(\alpha z^3) - I_{1/3}(\alpha z^3) \frac{I_{2/3}(\alpha z_0^3)}{I_{-2/3}(\alpha z_0^3)} \right], \quad (11)$$

where $\alpha = g_5 \sigma / 3$ (one may use here Airy functions instead of $I_{-1/3}(x), I_{2/3}(x)$, cf. [64]). The pion wave function $\Psi(z)$ coincides with the axial-vector bulk-to-boundary propagator $\mathcal{A}(0, z)$ taken at $p^2 = 0$. It is normalized by $\Psi(0) = 1$, satisfies Neumann boundary condition $\Psi'(z_0) = 0$ at the IR boundary and, due to the holographic correspondence, has the property that

$$f_\pi^2 = -\frac{1}{g_5^2} \left(\frac{1}{z} \partial_z \Psi(z) \right)_{z=\epsilon \rightarrow 0}. \quad (12)$$

For the neutral pion, it is convenient to define f_π through the matrix element of the σ_3 projection of the

axial-vector current

$$\langle 0 | J_\mu^{A,3} | \pi^0(p) \rangle \equiv \left\langle 0 \left| \frac{\bar{u} \gamma_\mu \gamma_5 u - \bar{d} \gamma_\mu \gamma_5 d}{2} \right| \pi^0(p) \right\rangle = i f_\pi p_\mu. \quad (13)$$

Then, the (experimental) numerical value of f_π is 92.4 MeV. Matching AdS₅ result $\Sigma^{\text{AdS}}(p^2) \sim \ln p^2 / (2g_5^2)$ and QCD result $\Sigma_3^{\text{QCD}}(p^2) \sim \ln p^2 / (8\pi^2)$ for the large- p^2 behavior of the correlator of $J_\mu^{A,3}$ currents gives $g_5 = 2\pi$ [43]. Analyzing pion EM form factor, one deals with charged pions, and the choice of the axial-vector current as $J_\mu^{A,(c)} = \bar{d} \gamma_\mu \gamma_5 u$ is more natural. Then $f_\pi^{(c)} = 130.7$ MeV, while $\Sigma_{(c)}^{\text{QCD}}(p^2) \sim \ln p^2 / (4\pi^2)$, hence, $g_5^{(c)} = \sqrt{2}\pi$ [69]. Of course, the combination $g_5^2 f_\pi^2$, be-

ing the ratio of the coefficient of the pion pole contribution $\Sigma_\pi(p^2) \sim f_\pi^2/p^2$ to the coefficient $\sim 1/g_5^2$ in $\Sigma(p^2)$'s large- p^2 behavior, remains intact:

$$g_5^2 f_\pi^2 = 4\pi^2 f_\pi^2 = 2\pi^2 (f_\pi^{(c)})^2 = (g_5^{(c)} f_\pi^{(c)})^2 \equiv s_0/2, \quad (14)$$

where $s_0 \approx 0.67 \text{ GeV}^2$. It is this convention-independent combination that enters Eq. (12).

Again, it is convenient to introduce the conjugate wave function [61]:

$$\Phi(z) = -\frac{1}{g_5^2 f_\pi^2} \left(\frac{1}{z} \partial_z \Psi(z) \right) = -\frac{2}{s_0} \left(\frac{1}{z} \partial_z \Psi(z) \right). \quad (15)$$

It vanishes at the IR boundary $z = z_0$, i.e., $\Phi(z_0) = 0$ and, according to Eq. (12), is normalized as $\Phi(0) = 1$ at the origin. From $\Phi(0) = 1$, it follows that the pion decay constant can be written as a function

$$g_5^2 f_\pi^2 = 3 \cdot 2^{1/3} \frac{\Gamma(2/3)}{\Gamma(1/3)} \frac{I_{2/3}(\alpha z_0^3)}{I_{-2/3}(\alpha z_0^3)} \alpha^{2/3} \quad (16)$$

of the condensate parameter α and the confinement radius z_0 . Note that the magnitude of α is independent of the g_5 -convention, while the value of σ depends on the g_5 -convention used.

After fixing z_0 through the ρ -meson mass, $z_0 = z_0^\rho = (323 \text{ MeV})^{-1}$, experimental f_π is obtained for $\alpha = (424 \text{ MeV})^3$. For these values, the argument $a \equiv \alpha z_0^3$ of the modified Bessel functions in Eq. (16) equals $2.26 \equiv a_0$. Since $I_{2/3}(a)/I_{-2/3}(a) \approx 1$ for $a \gtrsim 1$, then

$$g_5^2 f_\pi^2 \approx 3 \cdot 2^{1/3} \frac{\Gamma(2/3)}{\Gamma(1/3)} \alpha^{2/3}, \quad (17)$$

i.e., the value of f_π is basically determined by α alone (the same observation was made in the pioneering paper [45] and in a recent paper [64] in which the pion channel was studied numerically).

In Fig. 1, we illustrate the behavior of the pion wave functions Ψ and Φ representing them $\Psi \rightarrow \psi(\zeta, a)$, $\Phi \rightarrow \varphi(\zeta, a)$ as functions of dimensionless variables $\zeta \equiv z/z_0$ and $a \equiv \alpha z_0^3$. For $a = 0$ (i.e. when the chiral symmetry breaking parameter α vanishes), the limiting forms are $\psi(\zeta, 0) = 1$ and $\varphi(\zeta, 0) = 1 - \zeta^4$ [61]. As a increases, both functions become more and more narrow, with $\psi(\zeta, a)$ becoming smaller and smaller at the IR boundary $\zeta = 1$.

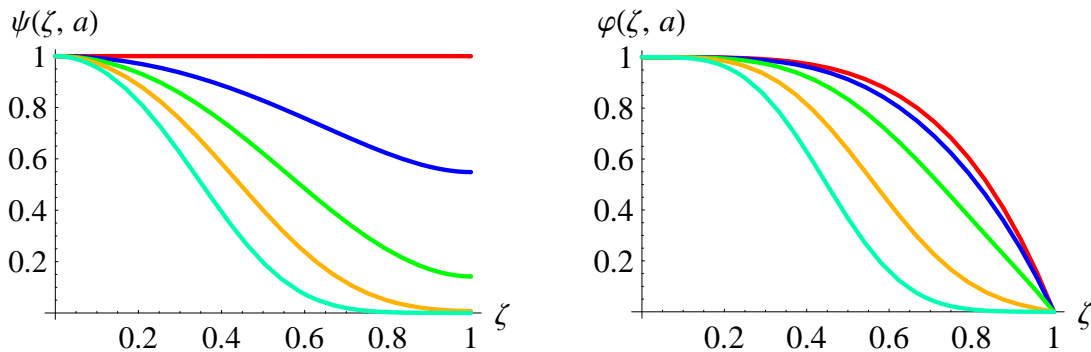


FIG. 1: Functions $\psi(\zeta, a)$ (left) and $\varphi(\zeta, a)$ (right) for several values of a : $a = 0$ (uppermost lines), $a = 1$, $a = 2.26$, $a = 5$, $a = 10$ (lowermost lines).

III. ANOMALOUS AMPLITUDE

A. Isosinglet fields

The $\pi^0 \gamma^* \gamma^*$ form factor is defined by

$$\begin{aligned} & \int \langle \pi, p | T \{ J_{EM}^\mu(x) J_{EM}^\nu(0) \} | 0 \rangle e^{-iq_1 x} d^4x \\ & = \epsilon^{\mu\nu\alpha\beta} q_{1\alpha} q_{2\beta} F_{\gamma^* \gamma^* \pi^0}(Q_1^2, Q_2^2), \end{aligned} \quad (18)$$

where $p = q_1 + q_2$ and $q_{1,2}^2 = -Q_{1,2}^2$. Its value for real photons

$$F_{\gamma^* \gamma^* \pi^0}(0, 0) = \frac{N_c}{12\pi^2 f_\pi} \quad (19)$$

is related in QCD to the axial anomaly.

Since π^0 meson is described by the third component A^3 of an isovector field, only the isovector component of the product of two electromagnetic currents gives nonzero contribution to the matrix element in Eq. (18). In QCD,

the electromagnetic current is given by the sum

$$J_\mu^{\text{EM}} = J_\mu^{\{I=1\},3} + \frac{1}{3} J_\mu^{\{I=0\}} \quad (20)$$

of isovector $J_\mu^{\{I=1\},a}(x)$ (“ ρ -type”) and isosinglet $J_\mu^{\{I=0\}}(x)$ (“ ω -type”) currents,

$$\begin{aligned} J_\mu^{\{I=1\},3} &= \frac{1}{2} (\bar{u}\gamma_\mu u - \bar{d}\gamma_\mu d) = \bar{q}\gamma_\mu t^3 q, \\ J_\mu^{\{I=0\}} &= \frac{1}{2} (\bar{u}\gamma_\mu u + \bar{d}\gamma_\mu d) = \frac{1}{2} \bar{q}\gamma_\mu \mathbb{1} q. \end{aligned} \quad (21)$$

As a result, the matrix element $\langle \pi^0 | J_\mu^{\text{EM}} J^{\text{EM}} | 0 \rangle$ is nonzero since it contains $\langle \pi^0 | J^{\{I=1\},3} J^{\{I=0\}} | 0 \rangle \sim \text{Tr}(t^3 t^3)$ parts.

To extract $F_{\gamma^* \gamma^* \pi^0}(Q_1^2, Q_2^2)$ form factor *via* holographic correspondence, we consider the correlator of the axial-vector current

$$J_\mu^{A,a} = \bar{q}\gamma_\mu \gamma_5 t^a q \quad (22)$$

and vector currents $J_\mu^{\{I=1\},b}, J_\nu^{\{I=0\}}$. To proceed, we need to have isoscalar fields on the AdS side of the holographic correspondence. This is achieved by gauging $U(2)_L \otimes U(2)_R$ rather than $SU(2)_L \otimes SU(2)_R$ group in the AdS/QCD action, i.e., by substituting $t^a B_\mu^a$ by

$$\mathcal{B}_\mu = t^a B_\mu^a + \mathbb{1} \frac{\hat{B}_\mu}{2} \quad (23)$$

in Eq. (2). Then the 4D currents correspond to the following 5D gauge fields

$$\begin{aligned} J_\mu^{A,a}(x) &\rightarrow A_\mu^a(x, z), \\ J_\mu^{\{I=0\}}(x) &\rightarrow \hat{V}_\mu(x, z), \\ J_\mu^{\{I=1\},a}(x) &\rightarrow V_\mu^a(x, z). \end{aligned} \quad (24)$$

B. Chern-Simons term

The terms contained in the original AdS/QCD action (2) cannot produce a 3-point function accompanied by the Levi-Civita $\epsilon^{\mu\nu\alpha\beta}$ factor. However, such a contribution may be obtained by adding the Chern-Simons (CS) term. We follow Refs. [65, 66] in choosing the form of the $\mathcal{O}(B^3)$ part of the $D = 5$ CS action (the only one we need). In the axial gauge $B_z = 0$, it is written as

$$\begin{aligned} S_{\text{CS}}^{(3)}[\mathcal{B}] &= k \frac{N_c}{48\pi^2} \epsilon^{\mu\nu\rho\sigma} \text{Tr} \int d^4x dz (\partial_z \mathcal{B}_\mu) \\ &\quad \times \left[\mathcal{F}_{\nu\rho} \mathcal{B}_\sigma + \mathcal{B}_\nu \mathcal{F}_{\rho\sigma} \right], \end{aligned} \quad (25)$$

where \mathcal{F} is the field-strength generated by \mathcal{B} and k should be an integer number adjusted to reproduce the QCD anomaly result. Then, in the $U(2)_L \otimes U(2)_R$ model, the relevant part of the CS term is [67]

$$S_{\text{CS}}^{\text{AdS}}[\mathcal{B}_L, \mathcal{B}_R] = S_{\text{CS}}^{(3)}[\mathcal{B}_L] - S_{\text{CS}}^{(3)}[\mathcal{B}_R]. \quad (26)$$

Taking into account that $\mathcal{B}_{L,R} = \mathcal{V} \pm \mathcal{A}$, and keeping only the longitudinal component of the axial-vector field $A \rightarrow A_\parallel$ (that brings in the pion), for which $F_{\mu\nu}^A = 0$, we have

$$\begin{aligned} S_{\text{CS}}^{\text{AdS}} &= k \frac{N_c}{24\pi^2} \epsilon^{\mu\nu\rho\sigma} \int d^4x \int_0^{z_0} dz \\ &\quad \times \left[(\partial_\rho V_\mu^a) \left(A_{\parallel\sigma}^a \overset{\leftrightarrow}{\partial}_z \hat{V}_\nu \right) + (\partial_\rho \hat{V}_\mu) \left(A_{\parallel\sigma}^a \overset{\leftrightarrow}{\partial}_z V_\nu^a \right) \right], \end{aligned} \quad (27)$$

where $\overset{\leftrightarrow}{\partial}_z \equiv \overset{\rightarrow}{\partial}_z - \overset{\leftarrow}{\partial}_z$. Representing $A_{\parallel\sigma}^a = \partial_\sigma \psi^a$ and integrating by parts gives

$$\begin{aligned} S_{\text{CS}}^{\text{AdS}} &= k \frac{N_c}{24\pi^2} \epsilon^{\mu\nu\rho\sigma} \int d^4x \int_0^{z_0} dz \\ &\quad \times \left[2(\partial_z \psi^a) (\partial_\rho V_\mu^a) (\partial_\sigma \hat{V}_\nu) - \psi^a \partial_z (\partial_\rho V_\mu^a \partial_\sigma \hat{V}_\nu) \right]. \end{aligned} \quad (28)$$

Note that the z -derivative of ψ^a is proportional to the Φ -function of the pion (15), which, as we argued in Refs. [60, 61, 69], is the most direct analog of the quantum-mechanical bound state wave functions, i.e., it is the derivative $\partial_z \psi^a(z)$ rather than $\psi^a(z)$ itself that is an analog of the pion 4D field. Then, the first term in the square brackets in Eq. (28) has the structure similar to the $\pi\omega\rho$ interaction term

$$\mathcal{L}_{\pi\omega\rho} = \frac{N_c g^2}{8\pi^2 f_\pi} \epsilon^{\mu\nu\alpha\beta} \pi^a (\partial_\mu \rho_\nu^a) (\partial_\alpha \omega_\beta), \quad (29)$$

obtained in the hidden local symmetries approach [70] from the anomalous Wess-Zumino [71, 72] lagrangian (see also a review [73]). Here g is the universal gauge coupling constant of that approach.

Integrating by parts over z , the second term of Eq. (28) can be also converted into a contribution of this form plus a $z = z_0$ surface term:

$$\begin{aligned} S_{\text{CS}}^{\text{AdS}} &= k \frac{N_c}{24\pi^2} \epsilon^{\mu\nu\rho\sigma} \int d^4x \left\{ - \left[\psi^a (\partial_\rho V_\mu^a) (\partial_\sigma \hat{V}_\nu) \right] \Big|_{z=z_0} \right. \\ &\quad \left. + 3 \int_0^{z_0} dz (\partial_z \psi^a) (\partial_\rho V_\mu^a) (\partial_\sigma \hat{V}_\nu) \right\}. \end{aligned} \quad (30)$$

The latter can be eliminated by adding a compensating surface term into the original Chern-Simons action, so that the resulting anomalous part of the action in the extended AdS/QCD model

$$\begin{aligned} S^{\text{anom}} &= k \frac{N_c}{8\pi^2} \epsilon^{\mu\nu\rho\sigma} \int d^4x \\ &\quad \times \int_0^{z_0} dz (\partial_z \psi^a) (\partial_\rho V_\mu^a) (\partial_\sigma \hat{V}_\nu) \end{aligned} \quad (31)$$

has the structure of Eq. (29).

C. Three-point function

The action (30) produces the 3-point function

$$\begin{aligned} \langle J_\alpha^{A,3}(-p) J_\mu^{\text{EM}}(q_1) J_\nu^{\text{EM}}(q_2) \rangle \\ = T_{\alpha\mu\nu}(p, q_1, q_2) i(2\pi)^4 \delta^{(4)}(q_1 + q_2 - p), \end{aligned} \quad (32)$$

with

$$T_{\alpha\mu\nu}(p, q_1, q_2) = \frac{N_c}{12\pi^2} \frac{p_\alpha}{p^2} \epsilon_{\mu\nu\rho\sigma} q_1^\rho q_2^\sigma K_b(Q_1^2, Q_2^2).$$

Here, p is the momentum of the pion and q_1, q_2 are the momenta of the photons.

The ‘‘bare’’ function $K_b(Q_1^2, Q_2^2)$ is given by

$$K_b(Q_1^2, Q_2^2) = -\frac{k}{2} \int_0^{z_0} \mathcal{J}(Q_1, z) \mathcal{J}(Q_2, z) \partial_z \psi(z) dz, \quad (33)$$

where $\mathcal{J}(Q_1, z)$, $\mathcal{J}(Q_2, z)$ are the vector bulk-to-boundary propagators (9), and $\psi(z)$ is the pion wave function (11).

D. Conforming to QCD axial anomaly

For real photons, i.e., when $Q_1^2 = Q_2^2 = 0$, the value of the $F_{\pi\gamma^*\gamma^*}(Q_1^2, Q_2^2)$ form factor in QCD (with massless quarks) is settled by the axial anomaly, which corresponds to $K^{\text{QCD}}(0, 0) = 1$. Our goal is to build an AdS/QCD model for $F_{\pi\gamma^*\gamma^*}(Q_1^2, Q_2^2)$ that reproduces this value. Taking $Q_1^2 = Q_2^2 = 0$, we have $\mathcal{J}(0, z) = 1$, and Eq. (33) gives

$$\begin{aligned} K_b(0, 0) &= -\frac{k}{2} \int_0^{z_0} \partial_z \psi(z) dz = -\frac{k}{2} \psi(z_0) \\ &= \frac{k}{2} \left[1 - \Psi(z_0) \right]. \end{aligned} \quad (34)$$

On the IR boundary $z = z_0$, the pion wave function $\Psi(z)$ from Eq. (11) is

$$\Psi(z_0) = \frac{\sqrt{3}\Gamma(2/3)}{\pi I_{-2/3}(a)} \left(\frac{1}{2a^2} \right)^{1/3}. \quad (35)$$

As we discussed above, experimental values of m_ρ and f_π correspond to $a = 2.26$, which gives $\Psi(z_0) = 0.14$. The magnitude of $\Psi(z_0)$ rapidly decreases for larger a (e.g., $\Psi(z_0)|_{a=4} \approx 0.02$, see Fig. 1). Still, the value of $\Psi(z_0)$ is nonzero at any finite value of a , and it is impossible to exactly reproduce the anomaly result by simply adjusting the integer number k . To conform to the QCD anomaly value $K^{\text{QCD}}(0, 0) = 1$, we add a surface term compensating the $\Psi(z_0)$ contribution in Eq. (34) and then take $k = 2$. To fix the form of the surface term, we note first that it should have the structure of a VVA 3-point function taken on the $z = z_0$ surface. Furthermore, using the derivatives $\mathcal{J}'_z(Q_i, z_0)$ of the bulk-to-boundary propagators in this term is excluded, because

$\mathcal{J}'_z(Q_i = 0, z_0) = 0$ at the real photon point. On the other hand, $\mathcal{J}(Q_i = 0, z_0) = 1$, and our final model for $F_{\pi\gamma^*\gamma^*}(Q_1^2, Q_2^2)$ corresponds to the function

$$\begin{aligned} K(Q_1^2, Q_2^2) &= \Psi(z_0) \mathcal{J}(Q_1, z_0) \mathcal{J}(Q_2, z_0) \\ &\quad - \int_0^{z_0} \mathcal{J}(Q_1, z) \mathcal{J}(Q_2, z) \partial_z \Psi(z) dz. \end{aligned} \quad (36)$$

The extra term provides $K(0, 0) = 1$, and since

$$\mathcal{J}(Q, z_0) = \frac{1}{I_0(Qz_0)}, \quad (37)$$

it rapidly decreases with the growth of Q_1 and/or Q_2 . We will see later that in these regions the behavior of $F_{\pi\gamma^*\gamma^*}(Q_1^2, Q_2^2)$ is determined by small- z region of integration. Thus, the effects of fixing the $\Psi(z_0) \neq 0$ artifact at the infrared boundary are wiped out in the ‘‘short-distance’’ regime.

IV. MOMENTUM DEPENDENCE

A. Small virtualities

If one of the photons is real $Q_1^2 = 0$, while another is almost real, $Q_2^2 = Q^2 \ll 1/z_0^2$, we may use the expansion

$$\mathcal{J}(Q, z) = 1 - \frac{1}{4} Q^2 z^2 \left[1 - \ln \frac{z^2}{z_0^2} \right] + \mathcal{O}(Q^4), \quad (38)$$

which gives (for $z_0 = z_0^p$ and $a = a_0 = 2.26$)

$$\begin{aligned} K(0, Q^2) &\simeq 1 - 0.66 \frac{Q^2 z_0^2}{4} \\ &\simeq 1 - 0.96 \frac{Q^2}{m_\rho^2}. \end{aligned} \quad (39)$$

The predicted slope is very close to the value $1/m_\rho^2$ expected from a naive vector-meson dominance. Experimentally, the slope of the $F_{\pi\gamma^*\gamma^*}(0, Q^2)$ form factor for small timelike (negative) Q^2 is measured through the Dalitz decay $\pi^0 \rightarrow e^+ e^- \gamma$. In our notations, the usual representation of the results is

$$K(0, Q^2) = 1 - a_\pi \frac{Q^2}{m_\pi^2}, \quad (40)$$

where m_π is the experimental pion mass. Then the Q^2 -slope given by Eq. (39) corresponds to $a_\pi \approx 0.031$. This number is not very far from the central values of two last experiments, $a_\pi = 0.026 \pm 0.024 \pm 0.0048$ [74], $a_\pi = 0.025 \pm 0.014 \pm 0.026$ [75], but the experimental errors are rather large. An earlier experiment [76] produced $a_\pi = -0.11 \pm 0.03 \pm 0.08$, a result whose central value has opposite sign and much larger absolute magnitude. In the spacelike region, the data are available only for the values $Q^2 \gtrsim 0.5 \text{ GeV}^2$ (CELLO [14]) and $Q^2 \gtrsim 1.5 \text{ GeV}^2$ (CLEO [15]) which cannot be treated as

very small. The CELLO collaboration [14] gives the value $a_\pi = 0.0326 \pm 0.0026$ that is very close to our result. To settle the uncertainty of the timelike data (and also on its own grounds), it would be interesting to have data on the slope from the spacelike region of very small Q^2 , which may be obtained by modification of the PRIMEX experiment [77] at JLab.

B. Large virtualities

Since $\mathcal{J}(Q, z_0)$ exponentially $\sim e^{-Qz_0}$ vanishes for large Q , we can neglect the first term of Eq. (36) in the asymptotic $Q^2 \rightarrow \infty$ region. Representing $\partial_z \psi(z)$ in terms of the $\Phi(z)$ wave function, we write $K(Q_1^2, Q_2^2)$ as

$$K(Q_1^2, Q_2^2) \simeq \frac{s_0}{2} \int_0^{z_0} \mathcal{J}(Q_1, z) \mathcal{J}(Q_2, z) \Phi(z) z dz . \quad (41)$$

Our goal is to compare the predictions based on this formula with the *leading-order* perturbative QCD results. Note that the situation is different from that with the charged pion form factor, where the leading-power $1/Q^2$ pQCD result $F_\pi^{\text{pQCD}}(Q^2) \rightarrow 2(\alpha_s/\pi) s_0/Q^2$ [11] corresponding to *hard* contribution is the $\mathcal{O}(\alpha_s)$ correction to the *soft* contribution, for which AdS/QCD gives $F_\pi^{\text{AdS/QCD}}(Q^2) \rightarrow s_0/Q^2$ [61]. In that situation, it makes no sense to discuss whether pQCD and AdS/QCD asymptotic predictions agree with each other numerically or not. In general, our AdS/QCD model contains no information about hard gluon exchanges of pQCD that produce the α_s factors. However, the pQCD expression for the $\gamma^* \gamma^* \rightarrow \pi^0$ form factor has *zero* order in α_s , so now it makes sense to compare the *leading-order* pQCD predictions for this particular (in fact, exceptional) form factor with AdS/QCD calculations.

It is instructive to consider first two simple kinematic situations ($Q_1^2 = 0, Q_2^2 = Q^2$ and $Q_1^2 = Q_2^2 = Q^2$), and then analyze the general case.

1. One real photon

Form factor in the kinematics when the virtuality of one of the photons can be treated as zero $Q_1^2 \approx 0$, while another $Q_2^2 = Q^2$ is large was studied experimentally by CELLO [14] and CLEO [15] collaborations.

In perturbative QCD, the $K(0, Q^2)$ form factor at large Q^2 is obtained from the factorization formula

$$K(0, Q^2) = \int_0^1 T(Q^2, x) \varphi_\pi(x) dx , \quad (42)$$

where $T(Q^2, x)$ is the amplitude of the hard subprocess $\gamma \gamma^* \rightarrow \bar{q}q$. The latter, modulo logarithms of Q^2 , has the $1/Q^2$ behavior. In the lowest order, when

$$K^{\text{pQCD}}(0, Q^2) = \frac{s_0}{3Q^2} \int_0^1 \frac{\varphi_\pi(x)}{x} dx \equiv \frac{s_0}{3Q^2} I^\varphi , \quad (43)$$

the purely $1/Q^2$ outcome reflects the large- Q^2 behavior of the hard quark propagator connecting the photon vertices. A particular form of the pion distribution amplitude (DA) is irrelevant to the power of the large- Q^2 behavior of $F(0, Q^2)$, as far as it provides a convergent x -integral in Eq. (43). The latter requirement is fulfilled, e.g., if the pion distribution amplitude $\varphi_\pi(x)$ vanishes at the end-points ($x = 0$ or 1) as a positive power of $x(1-x)$. Whether it vanishes at $x = 0$ as x, x^2 or \sqrt{x} does not matter – this would not affect the $1/Q^2$ large- Q^2 behavior of the $\gamma \gamma^* \pi^0$ form factor in the lowest pQCD order. However, the shape of the pion distribution amplitude $\varphi_\pi(x)$ determines the value of the coefficient I^φ that provides the normalization of the $\mathcal{O}(1/Q^2)$ term. For the asymptotic shape $\varphi_\pi^{\text{as}}(x) = 6x(1-x)$, we have $I^{\varphi^{\text{as}}} = 3$ and $K^{\text{pQCD}}(0, Q^2) = s_0/Q^2$.

Take now our extended AdS/QCD model for the $K(0, Q^2)$ form factor. It gives

$$K(0, Q^2) \simeq \frac{s_0}{2} \int_0^{z_0} \mathcal{J}(Q, z) \Phi(z) z dz . \quad (44)$$

At first sight, this expression, though completely different analytically from the pQCD formula (42), has a general structure similar to it: the Q^2 -dependence is accumulated in the universal current factor $\mathcal{J}(Q, z)$, while the bound state dynamics is described by the Q^2 -independent wave function $\Phi(z)$. The obvious difference is that the bulk-to-boundary propagator $\mathcal{J}(Q, z)$ does not have a power behavior at large Q^2 : it behaves in that region like e^{-Qz} , coinciding in this limit with $zQK_1(zQ) \equiv \mathcal{K}(Qz)$, the free-field version of the nonnormalizable mode. The *power behavior* in Q^2 appears only after integration of the *exponentially decreasing* function over z . As a result, only small values of z are important in the relevant integral, and the outcome is determined by the small- z behavior of the wave function $\Phi(z)$. As far as $\Phi(z)$ tends to a nonzero value $\Phi(0)$ when $z \rightarrow 0$, the outcome is the $1/Q^2$ behavior:

$$K(0, Q^2) \rightarrow \frac{\Phi(0)s_0}{2Q^2} \int_0^\infty d\chi \chi^2 K_1(\chi) = \frac{\Phi(0)s_0}{Q^2} . \quad (45)$$

Just like in the case of the (charged) pion EM form factor [61], the large- Q^2 behavior of $K(0, Q^2)$ is determined by the value of the $\Phi(z)$ wave function at the origin. Note, that this value is fixed: $\Phi(0) = 1$, which gives $K(0, Q^2) = s_0/Q^2$, the result that coincides with the leading-order prediction of pQCD for $I^\varphi = 3$, the value that is obtained, e.g., if one takes the asymptotic pion DA $\varphi_\pi^{\text{as}}(x) = 6x(1-x)$.

Experimentally, the leading-order pQCD prediction with $I^\varphi = 3$ is somewhat above the data. However, the next-to-leading $\mathcal{O}(\alpha_s)$ pQCD correction is negative, and decreases the result by about 15%, producing a satisfactory agreement. More elaborate fits [22] favor DAs that differ from the asymptotic one by higher Gegenbauer harmonics $x(1-x)C_n(2x-1)$ with $n = 2$ and $n = 4$. Still, for all the DAs obtained from these fits, the magnitude of the

integral I^φ is very close to the value $I^{\text{as}} = 3$ given by the asymptotic DA (see Ref. [22] for details and references). Thus, the result of our calculation is in full agreement with the magnitude of the leading-order pQCD part of the NLO fits of existing experimental data.

2. Equal virtualities

Another interesting kinematics is when the photons have equal large virtualities, $Q_1^2 = Q_2^2 = Q^2$. In this case, the leading-order pQCD prediction

$$K^{\text{pQCD}}(Q^2, Q^2) = \frac{s_0}{3} \int_0^1 \frac{\varphi_\pi(x) dx}{xQ^2 + (1-x)Q^2} = \frac{s_0}{3Q^2} \quad (46)$$

does not depend on the shape of the pion DA. In our extended AdS/QCD model, we obtain

$$K(Q^2, Q^2) \simeq \frac{s_0}{2} \int_0^{z_0} [\mathcal{J}(Q, z)]^2 \Phi(z) z dz . \quad (47)$$

Asymptotically, we have

$$K(Q^2, Q^2) \rightarrow \frac{\Phi(0)s_0}{Q^2} \int_0^\infty d\chi \chi^3 [K_1(\chi)]^2 = \frac{s_0}{3Q^2} , \quad (48)$$

which is the same result as in the leading-order pQCD.

3. General case

Finally, let us consider the general kinematics, when $Q_1^2 = (1+\omega)Q^2$, and $Q_2^2 = (1-\omega)Q^2$. The leading-order pQCD formula gives in this case

$$K^{\text{pQCD}}((1+\omega)Q^2, (1-\omega)Q^2) = \frac{s_0}{3Q^2} \int_0^1 \frac{\varphi_\pi(x) dx}{1+\omega(2x-1)} \equiv \frac{s_0}{3Q^2} I^\varphi(\omega) , \quad (49)$$

while Eq. (41) of our AdS/QCD model reduces, for large Q^2 , to

$$K((1+\omega)Q^2, (1-\omega)Q^2) \rightarrow \frac{\Phi(0)s_0}{2Q^2} \sqrt{1-\omega^2} \int_0^\infty d\chi \chi^3 K_1(\chi\sqrt{1+\omega}) K_1(\chi\sqrt{1-\omega}) \equiv \frac{s_0}{3Q^2} I^{\text{AdS}}(\omega) , \quad (50)$$

with the function $I^{\text{AdS}}(\omega)$ given by

$$I^{\text{AdS}}(\omega) = \frac{3}{4\omega^3} \left[2\omega - (1-\omega^2) \ln \left(\frac{1-\omega}{1+\omega} \right) \right] . \quad (51)$$

It is straightforward to check that $I^{\text{AdS}}(\omega)$ coincides with the pQCD function $I^\varphi(\omega)$ calculated for the asymptotic distribution amplitude $\varphi^{\text{as}}(x) = 6x(1-x)$. Indeed, using the representation

$$\chi K_1(\chi) = \int_0^\infty e^{-\chi^2/4u-u} du , \quad (52)$$

we can easily integrate over χ in Eq. (50) to get

$$K(Q_1^2, Q_2^2) \rightarrow \frac{s_0}{Q^2} \int_0^\infty \int_0^\infty \frac{u_1 u_2 e^{-u_1-u_2} du_1 du_2}{u_2(1+\omega) + u_1(1-\omega)} . \quad (53)$$

Changing variables $u_2 = x\lambda$, $u_1 = (1-x)\lambda$ and integrating over λ , we obtain

$$K(Q_1^2, Q_2^2) \rightarrow \frac{s_0}{3Q^2} \int_0^1 \frac{6x(1-x) dx}{1+\omega(2x-1)} , \quad (54)$$

which coincides with the pQCD formula (46) if we take $\varphi_\pi(x) = 6x(1-x)$.

Note that the absolute normalization of the asymptotic behavior of $K(Q_1^2, Q_2^2)$ for large Q_i in our model is fixed by the choice $k = 2$ that allows to conform to the value $K(Q_1^2, Q_2^2) = 1$ corresponding to the QCD anomaly result. As we have seen, this choice exactly reproduces also the leading-order pQCD result for the equal-virtualities form factor $K(Q^2, Q^2)$. The origin of this rather unexpected result needs further studies. Recall also that in pQCD the result for $K(Q^2, Q^2)$ is the same for any pion distribution amplitude, while the result for the unequal-virtualities form factor $K((1+\omega)Q^2, (1-\omega)Q^2)$ depends on the choice of the pion distribution amplitude. The fact that our AdS/QCD model gives the same result as the leading-order pQCD calculation performed for the asymptotic distribution amplitude, also deserves a further investigation.

4. From small to large Q^2

Both $K(0, Q^2)$ and $K(Q^2, Q^2)$ functions are equal to 1 at $Q^2 = 0$. For large Q^2 , the first one tends to s_0/Q^2 and the second one to $s_0/3Q^2$. The question is how these functions interpolate between the regions of small and large Q^2 . Long ago, Brodsky

and Lepage [8] proposed a simple monopole (BL) interpolation

$$K^{\text{BL}}(0, Q^2) = \frac{1}{1 + Q^2/s_0} \quad (55)$$

between the $Q^2 = 0$ value and the large- Q^2 asymptotic prediction of perturbative QCD for $K(0, Q^2)$. Later, this behavior was obtained within the ‘‘local quark-hadron duality’’ approach [27, 78], in which $K(0, Q^2)$ is obtained by integrating the spectral density $\rho(s, 0, Q^2) = Q^2/(s + Q^2)^2$ of the 3-point function over the ‘‘pion duality interval’’ $0 \leq s \leq s_0$. The curve for $Q^2 K(0, Q^2)$ based on Eq. (44) practically coincides with that based on BL interpolation (55), see Figs. 2 and 3. For comparison, we also show on Fig. 2 the monopole fit $K^{\text{CLEO}}(0, Q^2) = 1/(1 + Q^2/\Lambda_\pi^2)$ (with $\Lambda_\pi = 776$ MeV) of CLEO data [15]. As we mentioned, an accurate fit to CLEO data [22] was obtained in the next-to-leading order (NLO) pQCD, with the leading order part of the NLO pQCD fit being very close to BL-interpolation curve, and hence, to our AdS/QCD result as well.

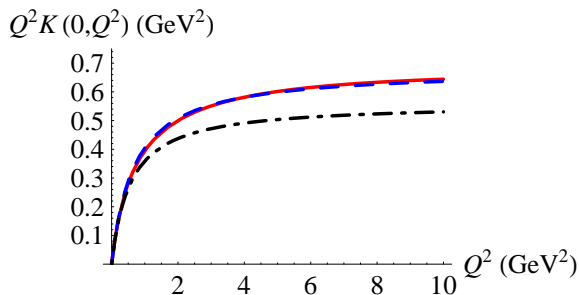


FIG. 2: Function $Q^2 K(0, Q^2)$ in AdS/QCD model (solid curve, red online) and in local quark hadron duality model (coinciding with Brodsky-Lepage interpolation formula, dashed curve, blue online). The monopole fit of CLEO data is shown by dash-dotted curve (black online).

In the case of $K(Q^2, Q^2)$ function, our model predicts the slope $1.92/m_\rho^2 \approx 2.15/s_0$ (twice the slope of $K(0, Q^2)$, see Eq. (39)), while the local duality model gives [27]

$$K^{\text{LD}}(Q^2, Q^2) = 1 - Q^4 \int_0^1 \frac{dx}{[Q^2 + s_0 x(1-x)]^2} \\ = 1 - \frac{2Q^2}{s_0 + 4Q^2} - \frac{8Q^4 \tanh^{-1} \sqrt{s_0/(s_0 + 4Q^2)}}{\sqrt{s_0(s_0 + 4Q^2)^3}}, \quad (56)$$

a curve which has the slope $2/s_0$ at $Q^2 = 0$:

$$K^{\text{LD}}(Q^2, Q^2) = 1 - 2 \frac{Q^2}{s_0} + \mathcal{O}(Q^4). \quad (57)$$

However, higher terms of Q^2 expansion become important for Q^2 as small as 0.01 GeV², where $K^{\text{AdS}}(Q^2, Q^2)$ becomes larger than $K^{\text{LD}}(Q^2, Q^2)$, and the ratio

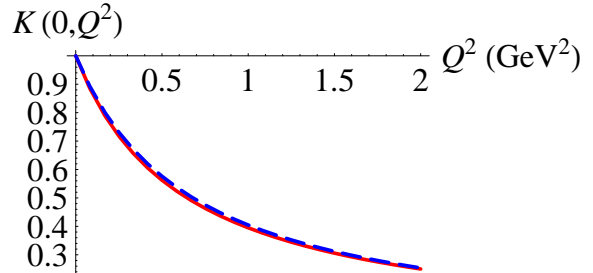


FIG. 3: Form factor $K(0, Q^2)$ in AdS/QCD model (solid curve, red online) compared to BL interpolation formula (dashed curve, blue online).

$K^{\text{AdS}}(Q^2, Q^2)/K^{\text{LD}}(Q^2, Q^2)$ reaches its maximum value of 1.08 for $Q^2 \sim 0.3$ GeV², then slowly decreasing towards the limiting value of 1. For large Q^2 , the local duality model gives the same result

$$K^{\text{LD}}(Q^2, Q^2) = \frac{s_0}{3Q^2} + \mathcal{O}(1/Q^4) \quad (58)$$

as our present model (48) and pQCD (46). As a consequence, our present model produces a curve that is very close to the curve based on the local duality model, see Fig. 4.

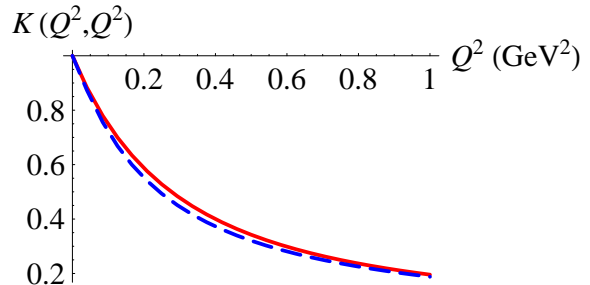


FIG. 4: Form factor $K(Q^2, Q^2)$ in AdS/QCD model (solid curve, red online) compared to the local quark-hadron duality model prediction (dashed curve, blue online).

V. BOUND-STATE DECOMPOSITION

The bulk-to-boundary propagator $\mathcal{J}(Q, z)$ may be written as a sum

$$\mathcal{J}(Q, z) = \sum_{n=1}^{\infty} \frac{g_5 f_n \psi_n^V(z)}{Q^2 + M_n^2} \quad (59)$$

over all vector bound states. For this reason, the form factor $K(Q_1^2, Q_2^2)$ also has a generalized vector meson dominance (GVMD) representation

$$K(Q_1^2, Q_2^2) = \sum_{n=1}^{\infty} \sum_{k=1}^{\infty} \frac{A_{n,k} + B_{n,k}}{(1 + Q_1^2/M_n^2)(1 + Q_2^2/M_k^2)}, \quad (60)$$

where $A_{n,k}$'s come from the first (surface) term in Eq.(36),

$$A_{n,k} = \frac{4\Psi(z_0)}{\gamma_{0,n}\gamma_{0,k}J_1(\gamma_{0,n})J_1(\gamma_{0,k})}, \quad (61)$$

while $B_{n,k}$'s are obtained from the second term and are given by the convolutions

$$B_{n,k} = -\frac{4}{z_0^2\gamma_{0,n}\gamma_{0,k}J_1^2(\gamma_{0,n})J_1^2(\gamma_{0,k})} \times \int_0^{z_0} \Psi'(z) J_1(\gamma_{0,n}z/z_0) J_1(\gamma_{0,k}z/z_0) z^2 dz. \quad (62)$$

Let us study the structure of the bound-state decomposition in two most interesting cases: for $K(0, Q^2)$ and $K(Q^2, Q^2)$.

A. One real photon

To study the bound-state decomposition of $K(0, Q^2)$, we write the basic expression

$$K(0, Q^2) = \Psi(z_0)\mathcal{J}(Q, z_0) - \int_0^{z_0} \mathcal{J}(Q, z) \Psi'(z) dz \quad (63)$$

and use GVMD representation (59) for $\mathcal{J}(Q, z)$. This gives

$$K(0, Q^2) = \sum_{n=1}^{\infty} \frac{A_n + B_n}{1 + Q^2/M_n^2}, \quad (64)$$

where

$$A_n = \frac{2\Psi(z_0)}{\gamma_{0,n}J_1(\gamma_{0,n})} \quad (65)$$

and B_n 's coincide with the coefficients

$$B_n = -\frac{2}{z_0\gamma_{0,n}J_1^2(\gamma_{0,n})} \int_0^{z_0} \Psi'(z) J_1(\gamma_{0,n}z/z_0) z dz \quad (66)$$

for the expansion

$$\Psi'(z) = -\frac{1}{z_0} \sum_{n=1}^{\infty} B_n \gamma_{0,n} J_1(\gamma_{0,n}z/z_0) \quad (67)$$

of the pion wave function $\Psi'(z)$ over the $\psi_n^V(z)/z$ wave functions (8) of vector meson bound states. In particular,

$$\begin{aligned} K(0, 0) &= \sum_{n=1}^{\infty} A_n + \sum_{n=1}^{\infty} B_n \\ &= \Psi(z_0) + [\Psi(0) - \Psi(z_0)] = 1. \end{aligned} \quad (68)$$

This relation may be directly obtained from the formula

$$2 \sum_{n=1}^{\infty} \frac{x J_1(\gamma_{0,n}x)}{\gamma_{0,n} J_1^2(\gamma_{0,n})} \Big|_{x \leq 1} = 1. \quad (69)$$

The bound state decomposition of $K(0, 0)$ looks like

$$K(0, 0) = 1 = 0.9512 + 0.0408 + 0.0446 - 0.0753 \quad (70) \\ + 0.0764 - 0.0736 + 0.0703 + \dots$$

There is a strong dominance of the lowest vector state, while each of the higher states is suppressed by more than factor of 10. The slow convergence of higher terms is due to A_n terms proportional to $\Psi(z_0) \approx 0.14$. For large n , one can approximate $A_n \approx \Psi(z_0)(-1)^n \sqrt{2/n}$.

Integrating by parts in Eq. (66) gives a representation directly for the total coefficient

$$A_n + B_n = \frac{2}{z_0^2 J_1^2(\gamma_{0,n})} \int_0^{z_0} \Psi(z) J_0(\gamma_{0,n}z/z_0) z dz, \quad (71)$$

that is related to the expansion of the pion wave function $\Psi(z)$ over the ϕ_n -functions (8) of vector meson bound states:

$$\Psi(z) = \sum_{n=1}^{\infty} (A_n + B_n) J_0(\gamma_{0,n}z/z_0). \quad (72)$$

Using it, one obtains again that $K(0, 0) = \Psi(0) = 1$. The slow convergence of higher terms in Eq. (70) is now explained by the necessity to reproduce the finite value of $\Psi(z)$ at $z = z_0$ by functions vanishing at $z = z_0$.

The slope of $K(0, Q^2)$ at $Q^2 = 0$ is given by the sum of $(A_n + B_n)/M_n^2$ coefficients, which converges rather fast:

$$K(0, Q^2) = 1 - \frac{Q^2}{m_\rho^2} \left\{ 0.9512 + 0.0077 + 0.0034 - 0.0031 \right. \\ \left. + 0.0020 - 0.0013 + 0.0009 + \dots \right\}, \quad (73)$$

and the contribution of the lowest state completely dominates the outcome.

Each term of the GVMD expansion (64) behaves like $1/Q^2$ at large Q^2 . In particular, the lowest-state contribution behaves like $0.95 m_\rho^2/Q^2 \approx (0.57 \text{ GeV}^2)/Q^2$. We also obtained above that $K(0, Q^2)$ behaves asymptotically like $s_0/Q^2 \approx (0.67 \text{ GeV}^2)/Q^2$. The two scales are not so different, and one may be tempted to speculate that the large- Q^2 behavior of $K(0, Q^2)$ also reflects the dominance of the lowest resonance. However, the coefficient of $1/Q^2$ is formally given by the sum of $(A_n + B_n)M_n^2$ terms, which does not show good convergence even after 7 terms are taken:

$$\sum_{n=1}^{\infty} (A_n + B_n)M_n^2 = m_\rho^2 \left\{ 0.951 + 0.215 + 0.577 \right. \\ \left. - 1.811 + 2.945 - 4.158 + 5.473 + \dots \right\}. \quad (74)$$

A simple comment is in order now: within the AdS/QCD model [43] the ρ -meson mass is determined by the “confinement radius” z_0 , while the scale $s_0 = 8\pi^2 f_\pi^2$ is basically determined by the chiral symmetry breaking parameter α (see Eq. (16) and preceding discussion). Calculationally, the coefficient s_0 of $1/Q^2$ asymptotic behavior was determined solely by the magnitude of the pion wave function $\Psi'(z)/z$ at the origin. Furthermore, it was legitimate to take the free-field form of the vector bulk-to-boundary propagator in our calculation, i.e., no information about vector channel mass scales was involved.

Moreover, one may write the bound-state decomposition for the $J(Q, z_0)$ function. Again, each term of such a decomposition has $1/Q^2$ asymptotic behavior, while $J(Q, z_0)$ *exponentially* decreases for large Q . In fact, the formal sum $\sum_n A_n M_n^2$ in this case diverges like $\sum_n (-1)^n n^{3/2}$.

Summarizing, the $1/Q^2$ asymptotic behavior of $K(0, Q^2)$ has nothing to do with the fact that the contribution of each particular bound state has $1/Q^2$ behavior. If, instead of $\Phi(z)$, one would take a function with $\sim z^\Delta$ behavior for small z , one would still be able to write the GVM representation for such a version of $K(0, Q^2)$, but its asymptotic behavior will be $\sim 1/Q^{2+\Delta}$.

B. Two deeply virtual photons

Each term of the bound-state decomposition (60) for $K(Q^2, Q^2)$ has $1/Q^4$ behavior. Thus, in the case of strong dominance of a few lowest states, one would expect $1/Q^4$ large- Q^2 behavior of this function.

However, as we already obtained, the function

$K(Q^2, Q^2)$ behaves like $1/Q^2$ for large Q^2 . This result was a consequence of two features of the form factor integral (41). The first is the fact that the bulk-to-boundary propagator $\mathcal{J}(Q, z)$ behaves like e^{-Qz} for large Q . This is a very general property: in this limit $\mathcal{J}(Q, z)$ should coincide with its free-field version $\mathcal{K}(Qz) = zQK_1(zQ)$. The second feature is that the pion wave function $\Phi(z)$ is finite at the origin, which follows from the basic formula (12) that defines f_π .

Hence, to qualitatively understand the mechanism that produces $1/Q^2$ result from the doubly-infinite sum of $1/Q^4$ terms, one may consider a simpler “toy” model that also has these general properties, but allows to analytically calculate integrals that determine the coefficients in Eq. (60). In particular, an explicit result for $K(Q_1^2, Q_2^2)$ may be obtained if we take the soft-model expression [69]

$$\mathcal{J}^s(Q, z) = a \int_0^1 x^{a-1} \exp\left[-\frac{x}{1-x} \kappa^2 z^2\right] dx \quad (75)$$

for the bulk-to-boundary propagators (with κ being the oscillator parameter and $a = Q^2/4\kappa^2$) and

$$\Psi^s(z) = e^{-\kappa^2 z^2} \quad (76)$$

for the pion wave function. This model has the required properties, namely, $\mathcal{J}^s(Q, z)$ approaches the free-field function $\mathcal{K}(Qz)$ for large Q^2 , while $\Phi(0)$ is finite.

Calculating the integral

$$K^s(Q_1^2, Q_2^2) = 2\kappa^2 \int_0^\infty \mathcal{J}^s(Q_1, z) \mathcal{J}^s(Q_2, z) e^{-\kappa^2 z^2} z dz \quad (77)$$

gives

$$K^s(Q_1^2, Q_2^2) = \sum_{n=0}^{\infty} \frac{a_1}{(a_1+n)(a_1+n+1)} \frac{a_2}{(a_2+n)(a_2+n+1)}, \quad (78)$$

where $a_1 = Q_1^2/M^2$, $a_2 = Q_2^2/M^2$ and $M = 2\kappa$ is the mass of the lowest bound state. The spectrum corresponding to $\mathcal{J}^s(Q, z)$ is given by $M_m^2 = mM^2$, with $m = 1, 2, \dots$, and Eq. (78) explicitly displays the bound state poles. For large Q_1^2, Q_2^2 , each term of this sum behaves like $1/Q_1^2 Q_2^2$. However, taking $a_1 = a_2 = a \gg 1$ gives

$$K^s(Q^2, Q^2) \rightarrow a^2 \int_0^\infty \frac{dn}{(n+a)^4} = \frac{1}{3a} = \frac{M^2}{3Q^2}. \quad (79)$$

Thus, the conversion from the $1/Q^4$ asymptotics of individual terms to the $1/Q^2$ asymptotics of the sum is due to nondecreasing $\mathcal{O}(n^0)$ behavior of the coefficients accompanying n^{th} term of the sum. In other words, transitions involving higher bound states are important, i.e., the pole decomposition is far from being dominated by a few lowest states.

C. Structure of two-channel pole decomposition

However, to make specific statements about the transitions, one should realize that Eq. (78) does not have the form of Eq. (60). In particular, it is not a double sum, and having a sum over a single parameter implies that the

summation parameters n and k in the double sum representation are correlated. A simple inspection of Eq. (78) shows that either $k = n$ or $k = n \pm 1$. Furthermore, the representation (78) has $Q_1^2 Q_2^2$ factor in the numerator, which should be canceled against the denominator factors to get an expression in which Q_1^2 and Q_2^2 appear in denominators only. The easiest way to obtain the desired GVMD-type expansion for $K^s(Q_1^2, Q_2^2)$ is to use another representation [69]

$$\mathcal{J}^s(Q, z) = \kappa^2 z^2 \int_0^1 \exp \left[-\frac{x}{1-x} \kappa^2 z^2 \right] \frac{x^a dx}{(1-x)^2} \quad (80)$$

for the bulk-to-boundary propagators. Then

$$K^s(Q_1^2, Q_2^2) = \sum_{n=0}^{\infty} \frac{(n+1)(n+2)}{(a_1+n+1)(a_1+n+2)(a_2+n+1)(a_2+n+2)}. \quad (81)$$

Now, each term of the sum decreases as $1/Q_1^4 Q_2^4$, but the sum may be rewritten as

$$K^s(Q_1^2, Q_2^2) = \sum_{n=1}^{\infty} \frac{1}{1+Q_1^2/M_n^2} \left\{ \frac{2}{1+Q_2^2/M_n^2} - \frac{1}{1+Q_2^2/M_{n+1}^2} - \frac{1}{1+Q_2^2/M_{n-1}^2} \right\}, \quad (82)$$

i.e., the coefficients $B_{n,k}^s$ of the bound-state expansion (60) in this model are given by

$$B_{n,k}^s = 2\delta_{n,k} - \delta_{n,k+1} - \delta_{n,k-1} \quad (83)$$

(there is no need to add surface terms in this model since $\Psi^s(\infty) = 0$, and hence $A_{n,k}^s = 0$).

When $Q_2^2 = 0$, only the $n = 1$ term contributes, and $K(Q^2, 0)$ in this model is formally dominated by the lowest resonance:

$$K^s(Q^2, 0) = \frac{1}{1+Q^2/M_1^2}. \quad (84)$$

This fact may create an impression that the $\pi^0 \rightarrow \gamma\gamma$ decay in this model is dominated by the $\rho\omega$ intermediate state. However, the outcome that the sums of bracketed terms are zero for $n \geq 2$ is a result of cancellation of the contribution of a diagonal transition that gives 2, and two off-diagonal transitions, each of which gives -1 .

In fact, the coefficients $B_{n,n}^s = 2$ of diagonal transitions do not depend on n , and their total contribution into $K^s(Q_1^2, Q_2^2)$ diverges. On the other hand, the coefficients $B_{n,n+1}^s = -1$ and $B_{n+1,n}^s = -1$ of subdiagonal transitions are negative, and also do not depend on n . The total contribution into $K^s(Q_1^2, Q_2^2)$ of each of $k = n+1$ or $k = n-1$ off-diagonal transitions also diverges. In such a situation, claiming the dominance of the lowest states contribution makes no sense.

In the hard-wall model, the diagonal coefficients $B_{n,n}$ decrease with n , and they are visibly larger than the neighboring off-diagonal ones (see Table I). Thus, one may say that, for small Q_1^2, Q_2^2 , the value of $K(Q_1^2, Q_2^2)$ is dominated by the lowest bound states (the coefficients $A_{n,n}$ also decrease with n , see Table II, asymptotically they behave like $2\Psi(z_0)/n$). However, the large- Q_1^2, Q_2^2

$k \setminus n$	1	2	3	4	5
1	0.7905	0.0272	-0.1331	0.0562	-0.0275
2	0.0272	0.2484	-0.0423	-0.0608	0.0287
3	-0.1331	-0.0423	0.1624	-0.0367	-0.0403
4	0.0562	-0.0608	-0.0367	0.1199	-0.0303
5	-0.0275	0.0287	-0.0403	-0.0303	0.0951

TABLE I: Coefficients $B_{n,k}$ in the hard-wall model.

$k \setminus n$	1	2	3	4	5
1	0.3641	-0.2420	0.1935	-0.1658	0.1474
2	-0.2420	0.1609	-0.1286	0.1102	-0.0980
3	0.1935	-0.1286	0.1028	-0.0881	0.0783
4	-0.1658	0.1102	-0.0881	0.0755	-0.0671
5	0.1474	-0.0980	0.0783	-0.0671	0.0597

TABLE II: Coefficients $A_{n,k}$ in the hard-wall model

expansion is given by

$$K(Q_1^2, Q_2^2) = \frac{M_1^4}{Q_1^2 Q_2^2} \sum_{n,k=1}^{\infty} \frac{M_n^2 M_k^2}{M_1^4} (A_{n,k} + B_{n,k}) + \dots, \quad (85)$$

i.e., one should deal with the coefficients

$$B_{n,k} \frac{M_n^2 M_k^2}{M_1^4} = B_{n,k} \frac{\gamma_{0,n}^2 \gamma_{0,k}^2}{\gamma_{0,1}^4} \quad \text{and} \quad A_{n,k} \frac{M_n^2 M_k^2}{M_1^4}, \quad (86)$$

the lowest of which are given in Tables III and IV. Again,

$k \setminus n$	1	2	3	4	5
1	0.7905	0.1433	-1.7236	1.3514	-1.0593
2	0.1433	6.8952	-2.8875	-7.6956	5.8234
3	-1.7236	-2.8875	27.2323	-11.4306	-20.1136
4	1.3514	-7.6956	-11.4306	69.3299	-28.0684
5	-1.0593	5.8234	-20.1136	-28.0684	141.2499

TABLE III: Coefficients $B_{n,k}M_n^2M_k^2/M_1^4$ in the hard-wall model.

$k \setminus n$	1	2	3	4	5
1	0.3641	-1.2751	2.5056	-3.9868	5.6816
2	-1.2751	4.4655	-8.775	13.9624	-19.8979
3	2.5056	-8.775	17.2437	-27.4374	39.1011
4	-3.9868	13.9624	-27.4374	43.6572	-62.216
5	5.6816	-19.8979	39.1011	-62.216	88.6642

TABLE IV: Coefficients $A_{n,k}M_n^2M_k^2/M_1^4$ in the hard-wall model

the coefficients increase with n and k producing divergent series, just like in the toy soft-like model. Note, that asymptotically the sum of A -type terms gives a contribution exponentially decreasing with Q_1 and/or Q_2 , i.e., much faster than the $\sim 1/Q^4$ asymptotic behavior of each particular transition. On the other hand, the sum of B -type terms gives a contribution that has $\sim 1/Q^2$ asymptotic behavior, i.e., it drops slower than $1/Q^4$.

The convergence situation may be different in the real-world QCD, in which higher resonances are broad, with the width increasing with n (or k). Then the diagonal and neighboring non-diagonal transitions strongly overlap for large n and may essentially cancel each other.

VI. SUMMARY

At the end of the pioneering paper [43], it was indicated that one of the future developments of the holographic models would be an incorporation of the 5D Chern-Simons term to reproduce the chiral anomaly of QCD. However, only relatively recently Ref. [67] discussed a holographic model of QCD that includes Chern-Simons term (see also [79]) and, furthermore, extends the gauged $SU(2)_L \otimes SU(2)_R$ flavor group to $U(2)_L \otimes U(2)_R$.

In the present paper, we develop an extension of the AdS/QCD model, similar in form to that proposed in [67], but adjusted to study the anomalous coupling of the neutral pion to two (in general, virtual) photons. The additional part of the gauge field in the 5D bulk is associated with the isoscalar vector current (related to ω -like mesons). The Chern-Simons term allows to reproduce the tensor structure of the anomalous form factor $F_{\gamma^*\gamma^*\pi^0}(Q_1^2, Q_2^2)$. To exactly reproduce the QCD anomaly result for real photons, we added contributions localized at the IR boundary $z = z_0$, and then studied

the momentum dependence of the $F_{\gamma^*\gamma^*\pi^0}(Q_1^2, Q_2^2)$ form factor in our model.

In particular, we calculated the slope of the form factor with one real and one slightly off-shell photon. Our result $a_\pi \approx 0.031$ for the parameter of the usual $F_{\gamma^*\gamma^*\pi^0}(0, Q^2) = F_{\gamma^*\gamma^*\pi^0}(0, 0)(1 - a_\pi Q^2/m_\pi^2)$ low- Q^2 experimental representation of the data is very close to the value $a_\pi = 0.0326 \pm 0.0026$ obtained by CELLO collaboration [14] from spacelike Q^2 measurements, and rather close to the central values $a_\pi \sim 0.024$ of two most recent experiments [74, 75] for timelike Q^2 .

Although the holographic model is expected to work for low energies, where QCD is in the strong coupling regime, we found it interesting to investigate the behavior of the model form factor also in the regions where at least one of the photon virtualities is large. For the case with one real and one highly virtual photon, we demonstrated that our AdS/QCD result is in full agreement with the magnitude of the leading-order part of the next-to-leading-order pQCD fits of existing experimental data. In the kinematics when both photons have equal and large virtualities we obtained the same result as in the leading-order pQCD. Finally, we considered the general case of unequal and large photon virtualities. In this case, the form factor has a nontrivial dependence on the ratio Q_1^2/Q_2^2 of photon virtualities. Our calculation shows that the final result of our AdS/QCD model *analytically* coincides with the pQCD expression calculated using the asymptotic distribution amplitude $\varphi_\pi^{\text{as}}(x) = 6x(1-x)$. This result is rather unexpected, because initial expressions for the form factor have very different structure. It should be noted that the absolute normalization of the form factor $K(Q_1^2, Q_2^2)$ in our model is fixed by adjusting its value to $K(0, 0) = 1$ at the real photon point, which allows to conform to the QCD axial anomaly. The outcome that this choice exactly reproduces the leading-order pQCD result for the equal-virtualities form factor $K(Q^2, Q^2)$ needs further studies, as well as our result that the ω -dependence of the unequal-virtualities form factor $K((1+\omega)Q^2, (1-\omega)Q^2)$ coincides with the leading-order pQCD result derived by assuming the asymptotic shape for the pion distribution amplitude.

The bulk-to-boundary propagators entering into AdS/QCD formulas for form factors have a generalized vector-meson-dominance (GVMD) decomposition. As a result, the form factors also can be written in GVMD form. We studied the interplay between the GVMD decomposition of form factors and their behavior for large photon virtualities. In the case of one real photon, the function $K(0, Q^2)$ asymptotically behaves like $1/Q^2$. However, we demonstrated that this behavior has nothing to do with the fact that each term of the GVMD expansion for $K(0, Q^2)$ also behaves like $1/Q^2$ for large Q^2 . In fact, a formal GVMD expression for the coefficient of the $1/Q^2$ term diverges. When both photons are highly virtual, each term of the GVMD expansion for $K(Q^2, Q^2)$ behaves like $1/Q^4$, while $K(Q^2, Q^2)$ has $1/Q^2$ asymptotic behavior. Thus, we observe that only in the

region of small photon virtualities it makes sense to talk about dominating role of the lowest states. In particular, for real photons, when $Q_1^2 = Q_2^2 = 0$, the lowest (“ $\rho\omega\pi$ ”) transition amplitude contributes 1.15 into the $K(0,0) = 1$ value, the excess being primarily cancelled by the neighboring non-diagonal transitions.

VII. ACKNOWLEDGMENTS

H.G. would like to thank C. D. Roberts and J. Goity for valuable comments, T. S. Lee, M. Vanderhaeghen,

J. Erlich and J. Harvey for stimulating discussions, J. P. Draayer and A. W. Thomas for support at Louisiana State University and Jefferson Laboratory.

This paper is authored by Jefferson Science Associates, LLC under U.S. DOE Contract No. DE-AC05-06OR23177. The U.S. Government retains a non-exclusive, paid-up, irrevocable, world-wide license to publish or reproduce this manuscript for U.S. Government purposes.

-
- [1] S. L. Adler, Phys. Rev. **177**, 2426 (1969); J. S. Bell and R. Jackiw, Nuovo Cim. A **60**, 47 (1969); J. S. Schwinger, Phys. Rev. **82**, 664 (1951).
- [2] J.M. Cornwall, Phys.Rev.Lett. **16**, 1174 (1966).
- [3] D. J. Gross and S. B. Treiman, Phys. Rev. D **4**, 2105 (1971).
- [4] S. J. Brodsky, T. Kinoshita and H. Terazawa, Phys. Rev. D **4**, 1532 (1971).
- [5] J. Parisi and P. Kessler, Lett. Nuovo Cim. **2**, 755 (1971).
- [6] M. Jacob and T. T. Wu, Phys. Lett. B **232**, 529 (1989).
- [7] G. P. Lepage and S. J. Brodsky, Phys. Rev. D **22**, 2157 (1980).
- [8] S. J. Brodsky and G. P. Lepage, Phys. Rev. D **24**, 1808 (1981).
- [9] G. P. Lepage, S. J. Brodsky, T. Huang and P. B. Mackenzie, “*Hadronic Wave Functions In QCD*”, Report CLNS-82-522 (1982), published in Proceedings of 1981 Banff Summer Inst. (1982)
- [10] V. L. Chernyak and A. R. Zhitnitsky, Phys. Rept. **112**, 173 (1984).
- [11] A. V. Efremov and A. V. Radyushkin, Phys. Lett. B **94**, 245 (1980).
- [12] A. V. Radyushkin, JINR-P2-10717 (1977); English translation: arXiv:hep-ph/0410276.
- [13] G. P. Lepage and S. J. Brodsky, Phys. Lett. B **87**, 359 (1979).
- [14] H. J. Behrend *et al.* [CELLO Collaboration], Z. Phys. C **49**, 401 (1991).
- [15] J. Gronberg *et al.* [CLEO Collaboration], Phys. Rev. D **57**, 33 (1998)
- [16] F. del Aguila and M. K. Chase, Nucl. Phys. B **193**, 517 (1981).
- [17] E. Braaten, Phys. Rev. D **28**, 524 (1983).
- [18] E. P. Kadantseva, S. V. Mikhailov and A. V. Radyushkin, Yad. Fiz. **44**, 507 (1986) [Sov. J. Nucl. Phys. **44**, 326 (1986)].
- [19] I. V. Musatov and A. V. Radyushkin, Phys. Rev. D **56**, 2713 (1997)
- [20] A. Khodjamirian, Eur. Phys. J. C **6**, 477 (1999)
- [21] A. Schmedding and O. I. Yakovlev, Phys. Rev. D **62**, 116002 (2000)
- [22] A. P. Bakulev, S. V. Mikhailov, A. V. Pimikov and N. G. Stefanis, arXiv:0710.2275 [hep-ph].
- [23] M. B. Voloshin, Preprint ITEP-8-1982.
- [24] V. A. Nesterenko and A. V. Radyushkin, Sov. J. Nucl. Phys. **38**, 284 (1983) [Yad. Fiz. **38**, 476 (1983)].
- [25] S. V. Mikhailov and A. V. Radyushkin, Sov. J. Nucl. Phys. **49**, 494 (1989) [Yad. Fiz. **49**, 794 (1988)].
- [26] H. Ito, W. W. Buck and F. Gross, Phys. Rev. C **45**, 1918 (1992).
- [27] A. V. Radyushkin, Acta Phys. Polon. B **26**, 2067 (1995)
- [28] I. V. Anikin, M. A. Ivanov, N. B. Kulimanova and V. E. Lyubovitskij, Z. Phys. C **65**, 681 (1995).
- [29] A. V. Radyushkin and R. Ruskov, Nucl. Phys. B **481**, 625 (1996)
- [30] P. Kroll and M. Raulfs, Phys. Lett. B **387**, 848 (1996); R. Jakob, P. Kroll and M. Raulfs, J. Phys. G **22**, 45 (1996)
- [31] V. V. Anisovich, D. I. Melikhov and V. A. Nikonov, Phys. Rev. D **55**, 2918 (1997)
- [32] D. Kekez and D. Klabucar, Phys. Lett. B **457**, 359 (1999)
- [33] I. V. Anikin, A. E. Dorokhov and L. Tomio, Phys. Part. Nucl. **31**, 509 (2000) [Fiz. Elem. Chast. Atom. Yadra **31**, 1023 (2000)].
- [34] P. Maris and P. C. Tandy, Phys. Rev. C **65**, 045211 (2002)
- [35] A. E. Dorokhov, M. K. Volkov and V. L. Yudichev, Phys. Atom. Nucl. **66**, 941 (2003) [Yad. Fiz. **66**, 973 (2003)]
- [36] B. W. Xiao and B. Q. Ma, Phys. Rev. D **71**, 014034 (2005)
- [37] E. Ruiz Arriola and W. Broniowski, Phys. Rev. D **74**, 034008 (2006)
- [38] J. M. Maldacena, Adv. Theor. Math. Phys. **2**, 231 (1998) [Int. J. Theor. Phys. **38**, 1113 (1999)]; S. S. Gubser, I. R. Klebanov and A. M. Polyakov, Phys. Lett. B **428**, 105 (1998); E. Witten, Adv. Theor. Math. Phys. **2**, 253 (1998)
- [39] J. Polchinski and M. J. Strassler, Phys. Rev. Lett. **88**, 031601 (2002); JHEP **0305**, 012 (2003)
- [40] H. Boschi-Filho and N. R. F. Braga, JHEP **0305**, 009 (2003); Eur. Phys. J. C **32**, 529 (2004)
- [41] S. J. Brodsky and G. F. de Téramond, Phys. Lett. B **582**, 211 (2004); G. F. de Téramond and S. J. Brodsky, Phys. Rev. Lett. **94**, 201601 (2005)
- [42] T. Sakai and S. Sugimoto, Prog. Theor. Phys. **113**, 843 (2005); **114**, 1083 (2006)
- [43] J. Erlich, E. Katz, D. T. Son and M. A. Stephanov, Phys. Rev. Lett. **95**, 261602 (2005)

- [44] J. Erlich, G. D. Kribs and I. Low, Phys. Rev. D **73**, 096001 (2006)
- [45] L. Da Rold and A. Pomarol, Nucl. Phys. B **721**, 79 (2005); JHEP **0601**, 157 (2006)
- [46] A. Karch, E. Katz, D. T. Son and M. A. Stephanov, Phys. Rev. D **74**, 015005 (2006)
- [47] C. Csaki and M. Reece, JHEP **0705**, 062 (2007)
- [48] T. Hambye, B. Hassanain, J. March-Russell and M. Schwelling, Phys. Rev. D **74**, 026003 (2006); *ibid.* **76**, 125017 (2007).
- [49] J. Hirn and V. Sanz, JHEP **0512**, 030 (2005); J. Hirn, N. Rius and V. Sanz, Phys. Rev. D **73**, 085005 (2006)
- [50] K. Ghoroku, N. Maru, M. Tachibana and M. Yahiro, Phys. Lett. B **633**, 602 (2006)
- [51] S. J. Brodsky and G. F. de Teramond, Phys. Rev. Lett. **96**, 201601 (2006)
- [52] N. Evans, A. Tedder and T. Waterson, JHEP **0701**, 058 (2007)
- [53] R. Casero, E. Kiritsis and A. Paredes, Nucl. Phys. B **787**, 98 (2007).
- [54] U. Gursoy and E. Kiritsis, JHEP **0802**, 032 (2008).
- [55] U. Gursoy, E. Kiritsis and F. Nitti, JHEP **0802**, 019 (2008).
- [56] O. Bergman, S. Seki and J. Sonnenschein, JHEP **0712**, 037 (2007).
- [57] J. Erdmenger, K. Ghoroku and I. Kirsch, JHEP **0709**, 111 (2007).
- [58] J. Erdmenger, N. Evans, I. Kirsch and E. Threlfall, arXiv:0711.4467 [hep-th].
- [59] A. Dhar and P. Nag, JHEP **0801**, 055 (2008).
- [60] H. R. Grigoryan and A. V. Radyushkin, Phys. Lett. B **650**, 421 (2007).
- [61] H. R. Grigoryan and A. V. Radyushkin, Phys. Rev. D **76**, 115007 (2007).
- [62] H. R. Grigoryan, Phys. Lett. B **662**, 158 (2008).
- [63] Z. Abidin and C. E. Carlson, arXiv:0801.3839 [hep-ph].
- [64] H. J. Kwee and R. F. Lebed, JHEP **0801**, 027 (2008).
- [65] E. Witten, Adv. Theor. Math. Phys. **2**, 253 (1998).
- [66] C. T. Hill, Phys. Rev. D **73**, 126009 (2006).
- [67] S. K. Domokos and J. A. Harvey, Phys. Rev. Lett. **99**, 141602 (2007).
- [68] S. S. Chern and J. Simons, Annals Math. **99**, 48 (1974).
- [69] H. R. Grigoryan and A. V. Radyushkin, Phys. Rev. D **76**, 095007 (2007).
- [70] T. Fujiwara, T. Kugo, H. Terao, S. Uehara and K. Yamawaki, Prog. Theor. Phys. **73**, 926 (1985).
- [71] J. Wess and B. Zumino, Phys. Lett. B **37**, 95 (1971).
- [72] E. Witten, Nucl. Phys. B **223**, 422 (1983).
- [73] U. G. Meissner, Phys. Rept. **161**, 213 (1988).
- [74] F. Farzanpay *et al.*, Phys. Lett. B **278**, 413 (1992).
- [75] R. Meijer Drees *et al.* [SINDRUM-I Collaboration], Phys. Rev. D **45**, 1439 (1992).
- [76] H. Fonvieille *et al.*, Phys. Lett. B **233**, 65 (1989).
- [77] A. Gasparian, et al. "A Precision Measurement of the Neutral Pion Lifetime via the Primakoff Effect", JLab proposal PR-02-103, <http://www.jlab.org/primex/>
- [78] V. A. Nesterenko and A. V. Radyushkin, Phys. Lett. B **115**, 410 (1982).
- [79] E. Katz and M. D. Schwartz, JHEP **0708**, 077 (2007) [arXiv:0705.0534 [hep-ph]].